Wnt5b-induced PCP/JNK Activation Promotes PD-L1 Expression and the Malignant Phenotype of Non-small Cell Lung Cancer

Guangping Wu
China Medical University
Yuan Luo
China Medical University
Yusai Xie
China Medical University
Yang Han
China Medical University
Di Zhang
China Medical University
Qiang Han
China Medical University
Xinran Zhao
China Medical University
Ye Qin
China Medical University
Qingchang Li
China Medical University
Enhua Wang
China Medical University
Huanyu Zhao (zhaohy@cmu.edu.cn)
Department of Pathology, The First Affiliated Hospital and College of Basic Medical Sciences, China
https://orcid.org/0000-0003-4041-5617

Research

Keywords: Wnt5b, Dvl-3, JNK, PD-L1, non-small cell lung cancer

Posted Date: September 14th, 2020

DOI: https://doi.org/10.21203/rs.3.rs-74120/v1

Title page

Title

Wnt5b-induced PCP/JNK activation promotes PD-L1 expression and the malignant phenotype of non-small cell lung cancer

Authors

Guangping Wu[1], Yuan Luo[1], Yusai Xie[1], Yang Han[1], Di Zhang[1], Qiang Han[1], Xinran Zhao[1], Ye Qin[1], Qingchang Li[1], Enhua Wang[1], Huanyu Zhao[1*]

[1] Department of Pathology, The First Affiliated Hospital and College of Basic Medical Sciences, China Medical University, Shenyang, China

[*] Corresponding author: Huanyu Zhao, Department of Pathology, The First Affiliated Hospital and College of Basic Medical Sciences, China Medical University; postal address: No. 155 Nanjing North Street, Heping District, Shenyang, Liaoning, 110001, China; telephone and fax numbers: 86-24-83282177; email: zhaohy@cmu.edu.cn

Abstract

Background: Wnt5b is noncanonical Wnt ligand, and programmed-death ligand 1 (PD-L1) is a targeted agent for immunotherapy, but the mechanism by which Wnt5b regulates PD-L1 expression in non-small cell lung cancer (NSCLC) is unclear.

Methods: Wnt5b and PD-L1 expressions were detected in NSCLC specimens by immunohistochemistry. The interrelationship connecting Wnt5b with PD-L1 was verified using dual-luciferase assay, immunofluorescence, coimmunoprecipitation, western blot, real-time PCR and xenograft tumor model.

Results: Wnt5b and PD-L1 expressions were positively correlated in NSCLC specimens. Five-year survival time in the group with their coexpression was significantly lower than that without coexpression. Under the effect of Wnt5b, Frizzled-3 (Fzd3) initiated Dishevellde-3 (Dvl-3) membrane recruitment via DEP domain by Dvl-3 phosphorylation, contributing to activate PCP/JNK signaling through the small GTPase Rac1, and then upregulate PD-L1 expression and promote the malignant phenotype of NSCLC in vivo and in vitro. After PD-L1 antibody treatment, Wnt5b induced tumor growth was inhibited significantly in xenograft tumor model.

Conclusion: We demonstrate a new signal transduction pathway: Wnt5b initiates Dvl-3 membrane recruitment via DEP domain by Fzd3 so as to promote Rac1–PCP/JNK–PD-L1 pathway, which provides a potential target for clinical intervention and immunotherapy in lung cancer.

Keywords: Wnt5b, Dvl-3, JNK, PD-L1, non-small cell lung cancer

Background

Lung cancer is the leading cause of death of malignant tumor in the world. The invasion and metastasis are most likely to occur in the early stage, leading to the poor prognosis of the patient [1, 2]. Therefore, seeking for new therapeutic target is helpful to improve the prognosis and treatment of this disease.

Wnt pathway is important for tumorigenesis, including canonical Wnt/β-catenin pathway and noncanonical Wnt pathway. Wnt/PCP (planar cell polarity) belongs to noncanonical Wnt pathway, contributing to tumor invasion and metastasis [3]. Wnt ligand is a highly conserved secreted glycoprotein including 19 members, and Wnt5b belongs to noncanonical Wnt ligand. It regulates Wnt/PCP pathway [4]. Wnt5b is associated with the malignant phenotype of lung adenocarcinoma [5, 6]. However, the molecular mechanism by which Wnt5b takes part in PCP pathway in NSCLC is still unclear.

Recently, the research on tumor microenvironment has become a hot topic, especially PD-1/PD-L1 (programmed cell death protein 1; programmed death-ligand 1) immune checkpoints [7]. PD-L1 expressed by cancer cells acts as an inhibitor of human T cell responses [8]. PD-1 is able to dampen autoimmunity in the peripheral effector phase of T-cell activation. The interaction of cancer cells expressing PD-L1 with T cells expressing PD-1 enables cancer cells to obtain immune escape [9]. So the regulatory mechanisms of PD-L1 expression in cancer cells are worth researching. PD-L1

expression in triple-negative breast cancer is regulated by Wnt signaling [10]. However, the regulatory mechanisms of PD-L1 expression by Wnt signaling in NSCLC has not been reported.

Dishevelled (Dvl, consists of Dvl-1, Dvl-2 and Dvl-3) is a scaffold protein in Wnt pathway [11, 12], including three domains: DIX, DEP and PDZ. Dvl-3 affect the malignant phenotype of NSCLC mainly through noncanonical Wnt pathway [13, 14]. As a major signaling cassette of the mitogen-activated protein kinase (MAPK), the c-Jun N-terminal kinase (JNK) takes part in Wnt/PCP signaling [15-17]. Previous study confirmed that Dvl-3 could activate JNK in NSCLC [13], and also JNK activation is crucial for PD-L1 regulation in ovarian cancer cells [18]. Frizzled (Fzd) family belongs to seven transmembrane receptors, including ten isoforms (Fzd1-10). It binds to Wnt ligand and then interacts with Dvl to promote the Dvl phosphorylation for downstream cascade reaction [19, 20].

In summarize, we speculate that Wnt5b may impact one or more domains of Dvl-3 via a specific Fzd isoform so as to active Wnt/PCP signaling and regulate PD-L1 expression in NSCLC. In this work, we examined the Wnt5b and PD-L1 expression in NSCLC specimens. NSCLC xenograft murine models induced by Wnt5b combination with an anti-mouse PD-L1 antibody were established to explore the efficacy of anti-PD-L1 therapy in NSCLC. And we aslo elucidated the mechanism by which Wnt5b regulates PD-L1 expression involved in Wnt/PCP pathway.

Methods

Patients and specimens

We collected 137 NSCLC specimens (average age: 60 years). From 2004 to 2014, these patients underwent surgery at the First Affiliated Hospital of China Medical University, and none of them received radiotherapy or chemotherapy before resection. Written informed consent was obtained from them. Work procedures were approved by the Institute Research Ethics Committee (No. 2016 [LS] 014, China Medical University). We obtained tumor specimens during surgical resection. Histologic subtype is based on the 2015 classification criteria to lung cancer of the World Health Organization [21]; tumor stage is based on the 2010 International Union of cancer TNM staging standards [22]. Complete follow-up data was available for all the patients. Clinicopathological information is in Table 1.

We aslo collected 22 fresh paired carcinoma and adjacent noncancerous tissues, which were immediately stored at −70°C for mRNA and protein extraction.

Immunohistochemistry

Experimental procedures were performed as previous studies [13]. We incubated tissue sections with Wnt5b antibody (1:50, Abcam, ab94914). The intensity of Wnt5b staining was scored as following: 0 (no staining), 1 (weak staining), 2 (moderate staining), or 3 (strong staining). The percentage scores of Wnt5b staining were assigned as following: 1 (1%–25%), 2 (26%–50%), 3 (51%–75%), and 4 (76%–100%). The above two scores were multiplied to give a final score: 0 to 12. The

scores of ≥4 were defined as Wnt5b overexpression (positive expression); the scores between 1 and 4 were defined as weak expression (negative expression). The informations of PD-L1 staining were in Supplemental materials and methods.

PD-L1 staining was performed by using the Dako automated staining platform according to the manufacturer's standard steps (Dako 22C3 PharmDx Assay, Dako Autostainer Link 48, Agilent, Santa Clara, CA, USA). We determined the PD-L1 expression in tumor cells by using Tumor Proportion Score (TPS). TPS was calculated as the percentage of at least 100 viable tumor cells with complete or partial membrane staining. The percentage of ≥50% was defined as PD-L1 positive expression; and that of＜50% was defined as PD-L1 positive expression.

Cell culture, reagents and plasmid reconstruction

HBE cell was from the American Type Culture Collection (ATCC) (Manassas, VA, USA), and NSCLC cell lines (A549, SPC, H157, H460, LTE) were from the Shanghai Cell Bank (Shanghai, China). They were authenticated by short tandem repeat DNA profiling. We cultured cells according to the instructions of the ATCC.

siRNA-Wnt5b (sc-155357), siRNA-Fzd1 (sc-39977), siRNA-Fzd2 (sc-39979), siRNA-Fzd3 (sc-39981), siRNA-Fzd4 (sc-39983), siRNA-Fzd5 (sc-39985), siRNA-Fzd6 (sc-39987), siRNA-Fzd7 (sc-39990), siRNA-Fzd8 (sc-39992), siRNA-Fzd9 (sc-39994), siRNA-Fzd10 (sc-39996) and siRNA-negative control (sc-37007) were purchased from Santa Cruz Biotechnology Inc. pGPU6-Wnt5b-shRNA and pGPU6-NC-shRNA were purchased from Genepharma

(Shanghai, China). ML141 (a cdc42 inhibitor) and NSC23766 (a Rac1 inhibitor) were purchased from R&D Systems (Minneapolis, MN, USA). SP600125 (JNK inhibitor) were purchased from Merck Millipore (Bedford, MA).

pCMV6-AC-GFP-Wnt5b (RG200847) was purchased from Origene (Rockville, MD, USA). The pMyc-cyto and pMyc-cyto-Dvl-3 were provided by Dr. Jun Liu (Department of Chemistry, The Scripps Research Institute, La Jolla, CA).

The mutant Dvl-3 plasmids include the deletion of the DIX domain of Dvl-3 (myc-ΔDIX-Dvl-3), the deletion of the PDZ domain of Dvl-3 (myc-ΔPDZ-Dvl-3), the deletion of the DEP domain of Dvl-3 (myc-ΔDEP-Dvl-3) and the deletion of the DEP and PDZ domains of Dvl-3(myc-ΔDEP+PDZ-Dvl-3). They were produced by RiboBio (Guangzhou, China).

RNA extraction and Real-time PCR

We used PrimeScript™ RT reagent Kit (TaKaRa, Dalian, China) to perform Real-time PCR according to manufacturer's instruction. The experimental steps are conducted as the previous study [13]. β-actin was normalized reference. The sequences of primers in this research were shown in Table S1.

Western blot and immunoprecipitation

The experimental steps are conducted as the previous study [13]. We separated the membrane and cytosolic proteins by using Membrane and Cytosol Protein Extraction kit according to manufacturer's instruction (Beyotime Institute of Biotechnology,

Haimen, China). Detailed information of the antibodies is in Table S2.

Immunofluorescence staining

The experimental steps are conducted as the previous study [13]. After being treated with corresponding factors, the cell line was incubated overnight with an antibody against myc (1:50).

Dual-luciferase assay

We plated cells in 24-well plate. After incubation for 24 h, we transfected the mixture of 100 ng ATF2 (Wnt/PCP signalling, Promega, Madison, WI), or 100 ng TopFlash and FopFlash (Addgene, Cambridge, MA, USA), and 10 ng Renilla (Promega) according to the instructions of Lipofectamine 2000 (Invitrogen, Carlsbad, USA). Cells were treated with the indicated factors in addition to transfection of corresponding luciferase reporter gene vector. After incubation for 48 h, dual-luciferase assay system (Promega) was performed to measure the luciferase activity according to the instructions of manufacturer. We used TopFlash/FopFlash to measure β-catenin-dependent Wnt activity and ATF2 luciferase to measure Wnt/PCP activity. The values of various luciferase activities were normalized with Renilla activity. We repeated all the experiments at least three times.

Transwell assay

Transwell membranes (8 μm pore polycarbonate membrane, in 24-well plates) were used. We used Matrigel (BD Bioscience) on the upper surface of the membrane in every well. In the upper chamber, we cultured the cells (3×10^5 cells) in 100 μL serum-free medium; in the lower chamber, we added the medium containing 10% FBS. After incubation for 20 h, we stained the cells with hematoxylin (Sigma). Ten fields (400 × magnification) of each filter were randomly selected under microscope for counting the number of the invaded cells.

Cell scratch experiment

We seeded cells in six-well plates. After being treated with corresponding factors, the well was scratched by a 100 μL pipette tip. At 1 h and 24 h time points, we measured the scratch width under the microscope at three separated sites. The experiments were performed for three times.

Cdc42 and Rac1 GTPase Activation Assay

Rac1/cdc42 activation assay kit (Sigma-Aldrich, Deisenhofen, Germany) was used in this study according to manufacturer's instructions. After the pulldown reaction with GST-PAK-PBD (p21 binding domain of p21 activated kinase) beads, the precipitated proteins binding to the beads were performed to take immunoblotting assay with Rac1/cdc42 monoclonal antibody. We aslo determined the total amount of Rac1 or cdc42 by Western blot using total cell lysates.

Colony formation and MTT assays

The experimental steps are conducted as the previous study [13]. The experiments were performed for three times.

Transplantation of tumor cells into nude mice

The mice were treated in accordance with the experimental animal ethics guidelines established by China Medical University. The Institutional Animal Research Committee of China Medical University approved this study. We purchased specific pathogen-free (SPF) BALB/c nude mice (four-week-old; female; 17.54 ± 0.68 g) from Charles River (Beijing, China). In animal center of our university, we housed the mice in a controlled room with free access to food and water available. The condition of the room is 12 h light/dark cycle, a temperature of 24 ± 2°C and (55 ± 10)% relative humidity. There were sterilised wood shavings in the cages of the mice. Before surgical treatment, the mice were anesthetized with by intraperitoneal injection of Pentobarbital Sodium (40mg/kg; Sigma Aldrich, St.Louis, USA). We conducted the experimental procedures in the SPF laboratory during light phases.

NSCLC cells (Wnt5b expression plasmid-transfected A549 cells; Wnt5b-shRNA-transfected SPC and H157 cells; corresponding vector-transfected control cells) suspended in 0.2 ml PBS were intravenously inoculated to the tail vein (2×10^6 cells per mouse) or subcutaneously inoculated into the right flank (5×10^6 cells per mouse). Volume calculation formula for calculating tumour volume: length x width^2 x 0.5. Animals were randomized in the 2 following treatment groups (n=5 in

each group): Wnt5b expression plasmid-transfection or Wnt5b-shRNA-transfection, corresponding vector-transfection. After inoculation for 6 weeks, these nude mice were killed by cervical dislocation and then autopsied for collecting tumours and lungs. Dissected tissue and organs were fixed in 4% formaldehyde and then embedded in paraffin. We cut them into 4-μm-thick sections and stained them with hematoxylin to observe under microscope.

For detecting the effect of PD-L1, we subcutaneously inoculated NSCLC cells into the right flank as above. Animals were randomized in the 2 groups (n=5 in each group). When tumor volume reached to 90–100 mm^3, mice were treated twice a week (10 mg/kg) for 3 weeks days as following: anti-mouse PD-L1 antibody (Bioxcell) in Group 1; IgG2b antibody (New Hampshire, USA, Bioxcell) in Group 2. The antibody was executed by intraperitoneal injection. Then whole tumor was removed for study.

Statistical analysis

SPSS 17.0 was used for all analyses in this study. Chi-squared test was used to calculate corresponding correlations. Kaplan–Meier analysis was used to demonstrate the survival time among different groups of patients. A two-tailed $P < 0.05$ was considered to be statistically significant.

Results

Wnt5b and PD-L1 corexpression in NSCLC is correlated with poor prognosis

Wnt5b expression in 137 NSCLC samples and 36 paired non-cancerous samples was

detected by immunohistochemistry. Negative Wnt5b expression was in the normal bronchial and alveolar epithelial cells; in contrast, 62.8% of NSCLC tissues (86/137) had positive Wnt5b expression (Fig. 1a, Table 1).

Additionally, we evaluated the Wnt5b expression in 22 fresh NSCLC tissues. Wnt5b mRNA and protein expressions were higher in NSCLC tissues than that in matched paracancerous tissues (22/22; Fig. 1b and Fig. S1a). Compare with the normal bronchial epithelial cell line HBE, Wnt5b had high expression in NSCLC cells (Fig. 1c).

Wnt5b overexpression was significantly associated with high TNM stage and lymph node metastasis in NSCLC (Table 1, $P<0.05$). Kaplan–Meier survival analysis revealed that the overall survival for patients with Wnt5b overexpression was significantly shorter than that without Wnt5b overexpression ($P<0.05$; Fig. 1d).

PD-L1 expression in NSCLC tissues was significantly higher than that in paired normal tissues (Fig. 1a); Wnt5b and PD-L1 expressions were positively correlated in NSCLC tissues ($r = 0.198$, $P<0.05$, Table 1). The overall survival for patients with Wnt5b and PD-L1 coexpression was significantly shorter than that without coexpression ($P<0.05$; Fig. 1e).

Wnt5b promotes the malignant phenotype of NSCLC cells

To verify the effect of Wnt5b on the biological function of NSCLC cells, we transfected A549 cell (low Wnt5b expression) with Wnt5b expression plasmid. Wnt5b overexpression promoted the cell invasiveness, colony formation, proliferation and

migration. And Wnt5b knockdown (siRNA-Wnt5b) inhibited cell invasiveness, colony formation, proliferation and migration in SPC and H157 cells (Fig. 2a–h; Fig. S1b and S2a–d).

To assess the effect of Wnt5b on the tumorigenesis, NSCLC cells were intravenously injected via the tail vein or subcutaneously injected into nude mice. Compared with the control group (CTL), the weight and volume of subcutaneously injected tumours were increased in the Wnt5b overexpression group, and Wnt5b knockdown (shRNA-Wnt5b) had the opposite effect (A549: CTL versus Wnt5b; weight, 0.52±0.05 g versus 1.31±0.11 g; volume, 0.54±0.08 cm^3 versus 1.43±0.13 cm^3. SPC: shNC versus shRNA-Wnt5b; weight, 0.99±0.11 g versus 0.59±0.12 g; volume, 1.18±0.13 cm^3 versus 0.59±0.06 cm^3; $P<0.05$) (Fig. 2i–n; Fig. S2e–g). Compared with the control group, Wnt5b overexpression increased intrapulmonary metastasis formation, and Wnt5b knockdown had the opposite effect (lung metastasis rate: A549, CTL versus Wnt5b, 1/4 versus 4/4; SPC, shNC versus shRNA-Wnt5b, 4/4 versus 1/4) (Fig. 2o–r and Fig. S2h–i). Therefore, Wnt5b might function as a positive regulator of the progression of NSCLC in vitro and in vivo.

Wnt5b activates the Wnt/PCP signaling in NSCLC cells

Wnt5b is involved in PCP/JNK signaling [23]. Herein, we carried out luciferase reporter assays with an ATF2 reporter system, which is a robust readout for JNK signaling in Xenopus embryos [24]. Wnt5b overexpression strongly activated the ATF2 luciferase reporter, whereas Wnt5b knockdown had the opposite effect (Fig. 3a).

And Wnt5b had no effect on canonical Wnt signaling (TopFlash/FopFlash for Wnt/β-catenin signaling, Fig. S3a).

Next we detected the key factors in the Wnt/PCP pathway. Small GTPases Rac1 and cdc42 are involved in Wnt/PCP signaling [25, 26]. Wnt5b overexpression significantly upregulated the protein levels of Rac1 and cdc42, and Wnt5b knockdown had the opposite effect (Fig. 3b). The mRNA expressions of Rac1 and cdc42 were also positively regulated by Wnt5b (Fig. S3b). And Wnt5b had no effect on target genes (c-myc and cyclin D1) of canonical Wnt signaling (Fig. 3b and Fig. S3c). Above results confirm that Wnt5b activates Wnt/PCP signaling.

Wnt5b promotes Dvl-3 phosphorylation through Fzd3 in NSCLC cells

Dvl-1 and Dvl-3 affect malignant phenotype of NSCLC through different Wnt pathway.[14] Herein, Wnt5b could enhance Dvl-3 phosphorylation, but had no influence on Dvl-1 phosphorylation (Fig. 3b). Dvl-3 could activate JNK signaling to promote the malignant phenotype of NSCLC [13]. This has great significance for Wnt/PCP signaling [17, 27].

The transmembrane receptor Fzd binds to Wnt ligand, and then transduces downstream signals to the nucleus via Dvl [28]. Wnt5b is a noncanonical Wnt ligand, and Dvl-3 plays an important role in noncanonical Wnt pathway [13]. It reminds us that there is complex interaction among Wnt5b, Fzd and Dvl-3. Coimmunoprecipitation assay confirmed this (Fig. 3c).

Fzd includes ten isoforms. Fzd3 and Fzd6 are involved in Wnt/PCP pathway [29, 30].

To verify the effect of Fzds on Wnt5b induced Dvl-3 phosphorylation, we cotransfected siRNA-Fzd1-10 with Wnt5b expression plasmid (GFP-Wnt5b) to A549 cell. Fzd3 knockdown significantly inhibited the Wnt5b induced Dvl-3 phosphorylation, as well as the activation of the ATF2 reporter (Fig. 3d, e). And other isoforms had not this effect (Fig. S4–5). Coimmunoprecipitation assay confirmed that Wnt5b interacted with Fzd3 and Dvl-3, but this interaction was significantly weakened by siRNA-Fzd3 (Fig. 3f–h and Fig. S6). So Wnt5b promoted Dvl-3 phosphorylation through Fzd3.

Dvl-3 DEP domain is necessary for Wnt5b-mediated Dvl-3 phosphorylation through Fzd3 on cell membrane and the malignant phenotype of NSCLC cell induced by Wnt5b

Dvl includes three domains: DIX, DEP and PDZ. Different domains affect different Wnt pathways [31, 32]. Binding of Fzd through Dvl DEP domain is necessary for Dvl membrane recruitment upon Wnt stimulation and the propagation of downstream signals [33-35]. Herein, we constructed the wild-type (WT) and mutant Dvl-3 plasmids (myc-tagged) to evaluate the effect of different Dvl-3 domains (Fig. 4a). Coimmunoprecipitation results showed that Dvl-3 DEP domain contributed to the interaction of Wnt5b with Fzd3 and Dvl-3. After cotransfection with myc-Dvl-3 plasmid and GFP-Wnt5b, Wnt5b was able to interact with Fzd3 and Dvl-3. However, this interaction was abrogated upon the deletion of DEP domain, as well as the deletion of both of DEP and PDZ domains, but not the deletion of DIX or PDZ

93 domain (Fig. 4b).

94 Next, we tested the effect of Dvl-3 domains on Wnt5b-mediated Dvl-3
95 phosphorylation. After cotransfection GFP-Wnt5b with myc-Dvl-3 plasmid, Wnt5b
96 was able to promote the phosphorylation of Dvl-3 and JNK. However, this effect is
97 significantly abrogated upon the deletion of Dvl-3 DEP domain, as well as the
98 deletion of both of DEP and PDZ domains, but not the deletion of DIX or PDZ
99 domain (Fig. 4c). Dvl-3 could activate JNK [13]. And we also found that JNK
100 phosphorylation induced by Wnt5b mainly depended on Dvl-3 DEP domain (Fig. 4c).
101 JNK is important for Wnt/PCP signaling [15-17]. We found that Wnt5b-mediated
102 ATF2 reporter activation also depended on Dvl-3 DEP domain, but not the PDZ/DIX
103 domain (Fig. S7). And we also detected the effect of Dvl-3 mutation on the malignant
104 phenotype of NSCLC cell induced by Wnt5b. The result showed that Wnt5b and
105 Dvl-3 transfection promoted the cell invasiveness, colony formation, proliferation and
106 migration. However, this effect was abrogated upon the deletion of DEP domain, as
107 well as the deletion of both of DEP and PDZ domains, but not the PDZ or DIX
108 domain (Fig. S8). Take together, Dvl-3 DEP domain is necessary for Wnt5b-mediated
109 Dvl-3 phosphorylation and the subsequent activation of PCP/JNK signaling, as well
110 as the malignant phenotype of NSCLC cell induced by Wnt5b.

111 Previous results confirmed that Fzd3 was important for Wnt5b induced Dvl-3
112 phosphorylation (Fig. 3d, e). To test the effect of Fzd3, we performed cell membrane
113 protein and cytoplasmic protein extraction kit and immunofluorescence. The result
114 confirmed that Wnt5b promoted Dvl-3 phosphorylation on the cell membrane. After

adding siRNA-Fzd3, Dvl-3 phosphorylation was significantly decreased (Fig. 5a and Fig. S9). Immunofluorescent images showed that Dvl-3 membrane expression was abrogated upon the DEP domain deletion, as well as the deletion of both of the DEP and PDZ domains, but not the PDZ or DIX domain (Fig. 5b). Above results indicated that Dvl-3 DEP domain is necessary for Wnt5b-mediated Dvl-3 phosphorylation through Fzd3 on the cell membrane.

Dvl-3 DEP domain is necessary for Wnt5b-mediated Rac1 activation and the subsequent activation of PCP/JNK signaling

Wnt ligands transduce signals by activating Dvl, which can activate Rac1 [36], a member of Rho family of small GTPase, and then activate downstream JNK signaling [37, 38]. JNK activation is related to cancer progression. Our previous studies confirmed that Dvl-3 could activate JNK signaling in NSCLC [13]. Herein, we found that Dvl-3 transfection promoted Rac1 activation (Fig. S10a). Wnt5b significantly promoted the phosphorylation of Dvl-3 and JNK (Fig. 4c). Wnt5b resulted in Rac1 activation, but this effect was abrogated upon Fzd3 knockout (Fig. 6a and Fig. S10b). And cotransfection GFP-Wnt5b with myc-Dvl-3 promoted Rac1 activation, but this effect was abrogated upon the deletion of Dvl-3 DEP domain, as well as the deletion of both the DEP and PDZ domains, but not the PDZ or DIX domain (Fig. 6b). However, the effect of Wnt5b mediated cdc42 activation is not affected by any domain deletion (Fig. S10c). The effect of Wnt5b mediated JNK activation was significantly inhibited by adding Rac1 inhibitor, but this effect is not affected by

cdc42 inhibitor (Fig. 6c). Above results indicated that Dvl-3 DEP domain is necessary for Wnt5b mediated Rac1 activation and the subsequent activation of PCP/JNK signaling.

Wnt5b is involved in PD-L1 induction through JNK

JNK could upregulate PD-L1 expression in malignant tumors [18, 39]. So we explored whether Wnt5b regulated PD-L1 through JNK signaling.

Wnt5b significantly upregulated PD-L1 expression. JNK phosphorylation was increased upon Wnt5b. However, Wnt5b induced PD-L1 upregulation was inhibited by JNK inhibitor (Fig. 6d). It confirmed that JNK was important for Wnt5b induced PD-L1 upregulation.

We also evaluated the effect of PD-L1 antibody in vivo. After anti-mouse-PD-L1 antibody treatment, Wnt5b induced tumorigenesis was inhibited significantly (A549: Wnt5b+anti-PD-L1 versus Wnt5b+negative control; weight, 0.58±0.05 g versus 1.37±0.13 g; volume, 0.57±0.09 cm^3 versus 1.46±0.08 cm^3; $P<0.05$) (Fig. 6e, f).

Discussion

Noncanonical Wnt/PCP pathways regulate tumourigenesis. Wnt5b belongs to noncanonical Wnt ligand, which is involved in PCP pathway [4]. Herein, we demonstrated that Wnt5b overexpression was directly correlated with high TNM stage, lymph node metastasis, and poor prognosis of NSCLC patients. And Wnt5b enhanced the malignant phenotype of NSCLC in vivo and in vitro. So Wnt5b might be a

159 prognosis factor of NSCLC. Wnt5b is able to enhance Wnt/PCP signaling in NSCLC
160 cells.
161 Wnt ligand binds to Fzd receptor and triggers signal cascade reaction in Wnt/PCP
162 pathway [40-42]. Fzd4 regulates arterial formation and organization via Wnt/PCP
163 signaling [43]. Fzd5 activates noncanonical Wnt pathway [44]. As a noncanonical
164 Wnt ligand, Wnt5a binds to Fzd3 and acivates downstream JNK pathway [45]. Fzd3
165 and Fzd6 control the polarity of developing skin via Wnt/PCP pathway [30]. The
166 binding of Wnt5a to Fzd3 activates noncanonical Wnt signaling [46, 47]. Wnt5a and
167 Wnt5b are the most similar in structure. Herein, we demonstrated that Wnt5b bound
168 to Fzd3 in NSCLC cells, and Wnt5b promoted Wnt/PCP signaling via Fzd3 in
169 NSCLC.
170 Dvl transduces different Wnt signals to downstream pathways via Fzd [28]. The PDZ
171 and DIX domains of Dvl are important for both canonical and noncanonical Wnt
172 pathways, whereas DEP domain acts on Wnt/PCP signaling [42, 48-49]. DEP domain
173 could activate JNK signaling, which is important for Wnt/PCP pathway [50, 51]. And
174 DEP domain is necessary for Dvl membrane localization; its deletion inhibits the Dvl
175 membrane localization and impairs PCP signaling [42, 48-49, 52]. Wnt ligands
176 transduce various signals to activate Dvl, which can activate downstream small
177 GTPase Rac1 [36, 53], and then activate downstream JNK signaling [37]. Herein, we
178 found that under the effect of Wnt5b ligand, Fzd3 receptor initiate Dvl-3 membrane
179 recruitment via DEP domain and then activate PCP/JNK signaling via Rac1 in
180 NSCLC cell.

Activated T-lymphocytes triggers tumor cell death, but tumor cells could avoid this immune process so as to proliferate, depending on the immune checkpoint pathway. As a T cell immune checkpoint, PD-1 mediates immunosuppression. PD-L1 is expressed on tumor cells [54]. The interaction between PD-1 and PD-L1 could inhibit T-cell responses and preclinical antitumor activity [55]. Therefore, the PD-L1 expression is a predictor of the response to immune checkpoint inhibitors and the survival of the patients [56]. JNK signaling contributes to the upregulation of PD-L1 expression in malignant tumors [18, 39]. Herein, Wnt5b and PD-L1 coexpression was significantly correlated with poor prognosis of NSCLC patients; Wnt5b upregulated PD-L1 through JNK signaling. And anti-mouse-PD-L1 antibody treatment inhibited Wnt5b induced tumorigenesis significantly. So we hypothesize that Wnt5b is involved in PD-L1 induction, in turn, influencing the immune response in human NSCLC.

Conclusion

Overall, Wnt5b and PD-L1 coexpression in NSCLC is significantly correlated with poor prognosis. And we propose a signal transduction pathway as illustrated in Fig. S11: Wnt5b might recruit Dvl-3 by DEP domain to the membrane via Fzd3 so as to promote Rac1–PCP/JNK signaling, leading to increased PD-L1 expression and the progression of NSCLC. This pathway may provide a novel insight for targeted therapy and immunotherapy of lung cancer patient.

Abbreviations

PD-L1: programmed-death ligand 1; NSCLC: non-small cell lung cancer; Fzd: Frizzled; SPF: specific pathogen-free; WT: wild-type; Dvl-3: Dishevelled-3; PCP: planar cell polarity; PD-1: programmed cell death protein 1; MAPK: mitogen-activated protein kinase; JNK: c-Jun N-terminal kinase; ATCC: American Type Culture Collection; AC: adenocarcinoma; SCC: squamous cell carcinoma.

Ethics approval and consent to participate

NSCLC tissue samples were obtained from the patients in the First Affiliated Hospital of China Medical University. Written informed consent was obtained from them. Work procedures were approved by the Institute Research Ethics Committee (No. 2016 [LS] 014, China Medical University).The animal experiments were conducted in accordance with the experimental animal ethics guidelines established by China Medical University. The Institutional Animal Research Committee of China Medical University approved this study.

Consent for publication

Not applicable

Availability of data and materials

All data generated or analyzed during this study are included in this published article and its supplementary information files.

Competing interests

The authors declare that they have no competing interests.

Funding

This work was supported by the National Natural Science Foundation of China (No.81602022); and the National Training Program of Innovation and Entrepreneurship for Undergraduates of China Medical University in 2019 (No.201910159201).

Authors' contributions

Guangping Wu: Conceptualization, writing - review & editing; Yuan Luo: Data curation, software; Yusai Xie: Data curation, investigation; Yang Han: Methodology, validation; Di Zhang: Data curation, investigation; Qiang Han: Software, investigation; Xinran Zhao: Software, data curation; Ye Qin: Data curation, resources; Qingchang Li: Supervision, investigation; Enhua Wang: Conceptualization, writing - review & editing; Huanyu Zhao: Conceptualization, data curation, formal analysis, writing - review & editing. All authors read and approved the final manuscript

Acknowledgements

We thank Dr. Weinan Li for his technical support.

References

1. Chen X, Guan X, Zhang H, Xie X, Wang H, Long J, et al. DAL-1 attenuates epithelial-to mesenchymal transition in lung cancer. J Exp Clin Cancer Res. 2015;34:3.

2. Lin G, Sun L, Wang R, Guo Y, Xie C. Overexpression of muscarinic receptor 3 promotes metastasis and predicts poor prognosis in non-small-cell lung cancer. J Thorac Oncol. 2014;9:170–8.

3. Luga V, Wrana JL. Tumor-stroma interaction: Revealing fibroblast-secreted exosomes as potent regulators of Wnt-planar cell polarity signaling in cancer metastasis. Cancer Res. 2013;73:6843–7.

4. Guo L, Yamashita H, Kou I, Takimoto A, Meguro-Horike M, Horike S, et al. Functional investigation of a non-coding variant associated with adolescent idiopathic scoliosis in zebrafish:elevated expression of the ladybird homeobox gene causes body axis deformation. PLoS Genet. 2016;12:e1005802.

5. Zhang Q, Fan H, Liu H, Jin J, Zhu S, Zhou L, et al. WNT5B exerts oncogenic effects and is negatively regulated by miR-5587-3p in lung adenocarcinoma progression. Oncogene. 2020;39:1484–97.

6. Kato S, Hayakawa Y, Sakurai H, Saiki I, Yokoyama S. Mesenchymal transitioned cancer cells instigate the invasion of epithelial cancer cells through secretion of WNT3 and WNT5B. Cancer Sci. 2014;105:281–9.

7. Feng M, Xiong G, Cao Z, Yang G, Zheng S, Song X, You L, Zheng L, Zhang T, Zhao Y. PD-1/PD-L1 and immunotherapy for pancreatic cancer. Cancer Lett. 2017;407:57–65.

8. Kim H, Khanna V, Kucaba TA, Zhang W, Ferguson DM, Griffith TS, et al. Combination of Sunitinib and PD-L1 Blockade Enhances Anticancer Efficacy of TLR7/8 Agonist-Based Nanovaccine. Mol Pharm. 2019;16:1200–10.

9. Woods DM, Sodré AL, Villagra A, Sarnaik A, Sotomayor EM, Weber J. HDAC Inhibition Upregulates PD-1 Ligands in Melanoma and Augments Immunotherapy with PD-1 Blockade. Cancer Immunol Res. 2015;3:1375–85.

10. Castagnoli L, Cancila V, Cordoba-Romero SL, Faraci S, Talarico G, Belmonte B, et al. WNT signaling modulates PD-L1 expression in the stem cell compartment of triple-negative breast cancer. Oncogene. 2019;38:4047–60.

11. Lee HJ, Shi DL, Zheng JJ. Conformational change of Dishevelled plays a key regulatory role in the Wnt signaling pathways. Elife. 2015;4:e08142.

12. Zhao H, Xie C, Lin X, Zhao Y, Han Y, Fan C, et al. Coexpression of IQ-Domain GTPase-Activating protein 1 (IQGAP1) and dishevelled (Dvl) is correlated with poor prognosis in non-small cell lung cancer. PLoS One. 2014;9:e113713.

13. Zhao H, Zhao Y, Jiang G, Zhang X, Zhang Y, Dong Q, et al. Dishevelled-3 activates p65 to upregulate p120-catenin transcription via a p38-dependent pathway in non-small cell lung cancer. Mol Carcinog. 2015;54 Suppl 1:E112–21.

14. Zhao Y, Yang ZQ, Wang Y, Miao Y, Liu Y, Dai SD, et al. Dishevelled-1 and dishevelled-3 affect cell invasion mainly through canonical and noncanonical Wnt

283 pathway, respectively, and associate with poor prognosis in nonsmall cell lung cancer.
284 Mol Carcinog. 2010;49:760–70.
285 15. Gómez-Orte E, Sáenz-Narciso B, Moreno S, Cabello J. Multiple functions of the
286 noncanonical Wnt pathway. Trends Genet. 2013;29:545–53.
287 16. Gao Q, Zhang J, Wang X, Liu Y, He R, Liu X, et al. The signalling receptor
288 MCAM coordinates apical-basal polarity and planar cell polarity during
289 morphogenesis. Nat Commun. 2017;8:15279.
290 17. Geetha-Loganathan P, Nimmagadda S, Fu K, Richman JM. Avian facial
291 morphogenesis is regulated by c-Jun N-terminal kinase/planar cell polarity (JNK/PCP)
292 wingless-related (WNT) signaling. J Biol Chem. 2014;289:24153–67.
293 18. Wang JJ, Siu MK, Jiang YX, Leung TH, Chan DW, Cheng RR, et al. Aberrant
294 upregulation of PDK1 in ovarian cancer cells impairs CD8+ T cell function and
295 survival through elevation of PD-L1. Oncoimmunology. 2019;8:e1659092.
296 19. Punchihewa C, Ferreira AM, Cassell R, Rodrigues P, Fujii N. Sequence
297 requirement and subtype specificity in the high-affinity interaction between human
298 frizzled and dishevelled proteins. Protein Sci. 2009;18:994–1002.
299 20. Curto J, Del Valle-Pérez B, Villarroel A, Fuertes G, Vinyoles M, Peña R, et al.
300 CK1ε and p120-catenin control Ror2 function in noncanonical Wnt signaling. Mol
301 Oncol. 2018;12:611–29.
302 21. Travis WD, Brambilla E, Nicholson AG, Yatabe Y, Austin JHM, Beasley MB, et
303 al. The 2015 World Health Organization Classification of Lung Tumors: impact of
304 genetic, clinical and radiologic advances since the 2004 classification. J Thorac Oncol.

2015;10:1243–60.

22. Goldstraw P. Updated staging system for lung cancer. Surg Oncol Clin North Am. 2011;20:655–66.

23. Cohen ED, Tian Y, Morrisey EE. Wnt signaling: an essential regulator of cardiovascular differentiation, morphogenesis and progenitor self-renewal. Development. 2008;135:789–98.

24. Ohkawara B, Niehrs C. An ATF2-based luciferase reporter to monitor non-canonical Wnt signalling in Xenopus embryos. Dev Dyn. 2011;240:188–94.

25. Chen ZS, Li L, Peng S, Chen FM, Zhang Q, An Y, et al. Planar cell polarity gene Fuz triggers apoptosis in neurodegenerative disease models. EMBO Rep. 2018;19:e45409.

26. Dollar G, Gombos R, Barnett AA, Sanchez Hernandez D, Maung SM, Mihály J, et al. Unique and overlapping functions of formins Frl and DAAM during ommatidial rotation and neuronal development in Drosophila. Genetics. 2016;202:1135–51.

27. Cheng XN, Shao M, Li JT, Wang YF, Qi J, Xu ZG, et al. Leucine repeat adaptor protein 1 interacts with Dishevelled to regulate gastrulation cell movements in zebrafish. Nat Commun. 2017;8:1353.

28. Lee M, Hwang YS, Yoon J, Sun J, Harned A, Nagashima K, et al. Developmentally regulated GTP-binding protein 1 modulates ciliogenesis via an interaction with Dishevelled. J Cell Biol. 2019;218:2659–76.

29. Ghimire SR, Deans MR. Frizzled3 and Frizzled6 Cooperate with Vangl2 to Direct Cochlear Innervation by Type II Spiral Ganglion Neurons. J Neurosci.

2019;39:8013–23.

30. Dong B, Vold S, Olvera-Jaramillo C, Chang H. Functional redundancy of frizzled 3 and frizzled 6 in planar cell polarity control of mouse hair follicles. Development. 2018;145:dev168468.

31. Mentink RA, Rella L, Radaszkiewicz TW, Gybel T, Betist MC, Bryja V, et al. The planar cell polarity protein VANG-1/Vangl negatively regulates Wnt/β-catenin signaling through a Dvl dependent mechanism. PLoS Genet. 2018;14:e1007840.

32. Gammons MV, Rutherford TJ, Steinhart Z, Angers S, Bienz M. Essential role of the Dishevelled DEP domain in a Wnt-dependent human-cell-based complementation assay. J Cell Sci. 2016;129:3892–902.

33. Jiang X, Charlat O, Zamponi R, Yang Y, Cong F. Dishevelled promotes Wnt receptor degradation through recruitment of ZNRF3/RNF43 E3 ubiquitin ligases. Mol Cell. 2015;58:522–33.

34. Wald JH, Hatakeyama J, Printsev I, Cuevas A, Fry WHD, Saldana MJ, et al. Suppression of planar cell polarity signaling and migration in glioblastoma by Nrdp1-mediated Dvl polyubiquitination. Oncogene. 2017;36:5158–67.

35. Strakova K, Kowalski-Jahn M, Gybel T, Valnohova J, Dhople VM, Harnos J, et al. Dishevelled enables casein kinase 1-mediated phosphorylation of Frizzled 6 required for cell membrane localization. J Biol Chem. 2018;293:18477-93.

36. Čajánek L, Ganji RS, Henriques-Oliveira C, Theofilopoulos S, Koník P, Bryja V, et al. Tiam1 regulates the Wnt/Dvl/Rac1 signaling pathway and the differentiation of midbrain dopaminergic neurons. Mol Cell Biol. 2013;33:59–70.

349 37. Zhuang X, Zhang H, Li X, Li X, Cong M, Peng F, et al. Differential effects on
350 lung and bone metastasis of breast cancer by Wnt signalling inhibitor DKK1. Nat Cell
351 Biol. 2017;19:1274–85.
352 38. Fukukawa C, Nagayama S, Tsunoda T, Toguchida J, Nakamura Y, Katagiri T.
353 Activation of the non-canonical Dvl-Rac1-JNK pathway by Frizzled homologue 10 in
354 human synovial sarcoma. Oncogene. 2009;28:1110–20.
355 39. Qian Y, Deng J, Geng L, Xie H, Jiang G, Zhou L, et al. TLR4 signaling induces
356 B7-H1 expression through MAPK pathways in bladder cancer cells. Cancer Invest.
357 2008;26:816–21.
358 40. Niehrs C. The complex world of WNT receptor signalling. Nat Rev Mol Cell Biol.
359 2012;13:767–79.
360 41. Yamanaka H, Moriguchi T, Masuyama N, Kusakabe M, Hanafusa H, Takada R, et
361 al. JNK functions in the non-canonical Wnt pathway to regulate convergent extension
362 movements in vertebrates. EMBO Rep. 2002;3:69–75.
363 42. Boutros M, Paricio N, Strutt DI, Mlodzik M. Dishevelled activates JNK and
364 discriminates between JNK pathways in planar polarity and wingless signaling. Cell.
365 1998;94:109–18.
366 43. Descamps B, Sewduth R, Ferreira Tojais N, Jaspard B, Reynaud A, Sohet F, et al.
367 Frizzled 4 regulates arterial network organization through noncanonical Wnt/planar
368 cell polarity signaling. Circ Res. 2012;110:47–58.
369 44. Slater PG, Ramirez VT, Gonzalez-Billault C, Varela-Nallar L, Inestrosa NC.
370 Frizzled-5 receptor is involved in neuronal polarity and morphogenesis of

371 hippocampal neurons. PLoS One. 2013;8:e78892.
372 45. Jang S, Cho HH, Park JS, Jeong HS. Non-canonical Wnt mediated neurogenic
373 differentiation of human bone marrow-derived mesenchymal stem cells. Neurosci Lett.
374 2017;660:68–73.
375 46. Xie J, Zhao T, Liu Y. Sonic hedgehog regulates the pathfinding of descending
376 serotonergic axons in hindbrain in collaboration with Wnt5a and secreted
377 frizzled-related protein 1. Int J Dev Neurosci. 2018;66:24–32.
378 47. Onishi K, Shafer B, Lo C, Tissir F, Goffinet AM, Zou Y. Antagonistic functions of
379 Dishevelleds regulate Frizzled3 endocytosis via filopodia tips in Wnt-mediated
380 growth cone guidance. J Neurosci. 2013;33:19071–85.
381 48. Simons M, Gault WJ, Gotthardt D, Rohatgi R, Klein TJ, Shao Y, et al.
382 Electrochemical cues regulate assembly of the Frizzled/Dishevelled complex at the
383 plasma membrane during planar epithelialpolarization. Nat Cell Biol.
384 2009;11:286–94.
385 49. Wong HC, Mao J, Nguyen JT, Srinivas S, Zhang W, Liu B, et al. Structural basis
386 of the recognition of the dishevelled DEP domain in the Wnt signaling pathway. Nat
387 Struct Biol. 2000;7:1178–84.
388 50. Wallingford JB, Habas R. The developmental biology of Dishevelled: an
389 enigmatic protein governing cell fate and cell polarity. Development.
390 2005;132:4421–36.
391 51. Wang L, Wang C, Tao Z, Zhao L, Zhu Z, Wu W, et al. Curcumin derivative WZ35
392 inhibits tumor cell growth via ROS-YAP-JNK signaling pathway in breast cancer. J

Exp Clin Cancer Res. 2019;38:460.

52. Rothbächer U, Laurent MN, Deardorff MA, Klein PS, Cho KW, Fraser SE. Dishevelled phosphorylation, subcellular localization and multimerization regulate its role in early embryogenesis. EMBO J. 2000;19:1010–22.

53. Ma MZ, Zhuang C, Yang XM, Zhang ZZ, Ma H, Zhang WM, et al. CTHRC1 acts as a prognostic factor and promotes invasiveness of gastrointestinal stromal tumors by activating Wnt/PCP-Rho signaling. Neoplasia. 2014;16:265–78, 278.e1–13.

54. Topalian SL, Drake CG, Pardoll DM. Targeting the PD-1/B7-H1(PD-L1) pathway to activate anti-tumor immunity. Curr Opin Immunol. 2012;24:207–12.

55. Iwai Y, Ishida M, Tanaka Y, Okazaki T, Honjo T, Minato N. Involvement of PD-L1 on tumor cells in the escape from host immune system and tumor immunotherapy by PD-L1 blockade. Proc Natl Acad Sci U S A. 2002;99:12293–7.

56. El-Osta HE, Mott FE, Burt BM, Wang DY, Sabichi AL. Predictors of benefits from frontline chemoimmunotherapy in stage IV non-small-cell lung cancer: a meta-analysis. Oncoimmunology. 2019;8:e1665974.

Figure legends

Fig. 1. The expression of Wnt5b in NSCLC tissues and cell lines. (**a**) Wnt5b staining in normal bronchial epithelial cells, alveolar epithelial cells, squamous cell carcinoma (SCC) and adenocarcinoma (AC); PD-L1 staining in SCC and AC (magnification: ×400; scale bar, 20 μm). (**b**) Quantification of Wnt5b mRNA levels in human NSCLC

specimens and paired normal lung tissues by real-time PCR. (**c**) Wnt5b protein expression in five NSCLC cell lines and the normal bronchial cell line HBE. (**d**) The survival time of patients with Wnt5b-negative staining (I) and Wnt5b-positive staining (II). (**e**) The survival time of patients without Wnt5b and PD-L1 coexpression (I) and that of patients with coexpression (II). *, P<0.05.

Fig. 2. The influence of Wnt5b on the biological behavior of NSCLC cells. Colony formation (**a, b**), invasiveness (**c, d**), proliferation (**e, f**) and migration (**g, h**) of A549 and SPC cells; CTL, control, empty vector, the control group of Wnt5b expression plasmid. siWnt5b: siRNA-Wnt5b. siCTL, siRNA-control selected as a negative control. (**i-n**) Subcutaneously injected tumours (G418 screening, n=5). (**o-r**) Intravenously injection tumours (G418 screening, n=5). The arrow points to the cancerous area. Columns: mean numbers. shWnt5b, shRNA-Wnt5b. shNC, shRNA-negative control. *, P<0.05.

Fig. 3. The impact of Wnt5b on the Wnt/PCP pathway. (**a**) Dual-luciferase assay analyses of Wnt/PCP signaling. Transfection of siRNA-Wnt5b (siWnt5b) or Wnt5b expression plasmid (Wnt5b) to NSCLC cells. ATF2 luciferase was used to measure Wnt/PCP activity, and the values of luciferase activities were normalized with renilla activity. (**b**) Western blot analyses of target proteins; transfection of siWnt5b or Wnt5b to NSCLC cells; p-Dvl-1, Dvl-1 phosphorylation; p-Dvl-3, Dvl-3 phosphorylation. (**c**) Coimmunoprecipitation analyses of endogenous interaction

437 between Wnt5b, Fzd and Dvl-3 in A549. (**d**) Western blot analyses of Dvl-3
438 phosphorylation. (**e**) Dual-luciferase assay analyses of Wnt/PCP signaling;
439 cotransfection of siRNA-Fzd3 (siFzd3) with GFP-Wnt5b. (**f-g**)
440 Coimmunoprecipitation analyses of endogenous interaction between Wnt5b, Fzd3 and
441 Dvl-3 in A549 and SPC. (**h**) Coimmunoprecipitation analyses of the interaction of
442 Wnt5b with Dvl-3 in A549; cotransfection of siFzd3 with GFP-Wnt5b and myc-Dvl-3
443 plasmids. β-actin or GAPDH was selected as a control. siCTL, siRNA-control. *, P
444 <0.05.
445
446 **Fig. 4.** Wnt5b interacted with Dvl-3 DEP domain to promote Dvl-3 phosphorylation
447 and JNK activation. (**a**) The WT Dvl-3 plasmid and mutant Dvl-3 plasmids (△: this
448 domain deletion). (**b**) Coimmunoprecipitation analyses of the interaction of Wnt5b
449 with Fzd3 and Dvl-3; the resultant cell lysates were immunoprecipitated with
450 GFP/myc/Fzd3 antibody; the presence of Wnt5b/Dvl-3/Fzd3 was confirmed by
451 anti-GFP/myc/Fzd3 immunoblotting. (**c**) Western blot analyses of Dvl-3 and JNK.
452 Cotransfection of GFP-Wnt5b with WT myc-Dvl-3 or Dvl-3 mutant plasmids to A549
453 cell; p-Dvl-3, Dvl-3 phosphorylation; p-JNK, JNK phosphorylation. β-actin was
454 selected as a negative control. △DE+PD: △DEP+PDZ.
455
456 **Fig. 5**. The effect of Wnt5b on Dvl-3 membrane recruitment. (**a**) Western blot
457 analyses of Dvl-3 phosphorylation on cell membrane and cytoplasm; cotransfection of
458 siRNA-Fzd3 (siFzd3) with Wnt5b expression plasmid (Wnt5b) to A549 or

siRNA-Wnt5b (siWnt5b) with Wnt5b to SPC for 48 h. CTL, control, empty vector, the control group of Wnt5b expression plasmid; siCTL, siRNA-control. p-Dvl-3, Dvl-3 phosphorylation. Na-K ATPase was a reference control for membrane. (**b**) Analysis of Dvl-3 localization with confocal microscopy (magnification: ×400); cotransfection of GFP-Wnt5b with WT myc-Dvl-3 or Dvl-3 mutant plasmids for 48 h to A549 cell.

Fig. 6. The impact of Wnt5b on Rac1, JNK and PD-L1. (**a**) Western blot analyses of activated Rac1; cotransfection of siRNA-Fzd3 (siFzd3) with Wnt5b expression plasmid (Wnt5b) or siRNA-Wnt5b (siWnt5b). (**b**) Western blot analyses of Rac1 in A549 cell; cotransfection of GFP-Wnt5b with WT myc-Dvl-3 or Dvl-3 mutant plasmids. (**c**) Western blot analyses of Rac1, cdc42 and JNK. P-JNK, JNK phosphorylation; transfection of GFP-Wnt5b (Wnt5b) to A549 cell. After Wnt5b transfection, NSC23766 (a Rac1 inhibitor, 100 μM, Wnt5b+NSC) or ML141 (a cdc42 inhibitor, 10 μM, Wnt5b+ML141) was treated for 24 h. Whole-cell lysates were run on parallel gels to determine total Rac1 or cdc42. (**d**) Western blot analyses of PD-L1 and JNK; transfection of GFP-Wnt5b (Wnt5b) to A549. After Wnt5b transfection, SP600125 (JNK inhibitor, 10 μM, Wnt5b+SP) was treated for 24 h. (**e-g**) Subcutaneously injected tumours of A549 cell stably expressing Wnt5b (G418 screening, n=5) with PD-L1 antibody treatment. CTL, control, empty vector, the control group of Wnt5b expression plasmid; siCTL, siRNA-control. β-actin was

480 selected as a negative control. W+N, Wnt5b+negative control for PD-L1 antibody;

481 W+P, Wnt5b+PD-L1 antibody. *, P <0.05.

482

Figures

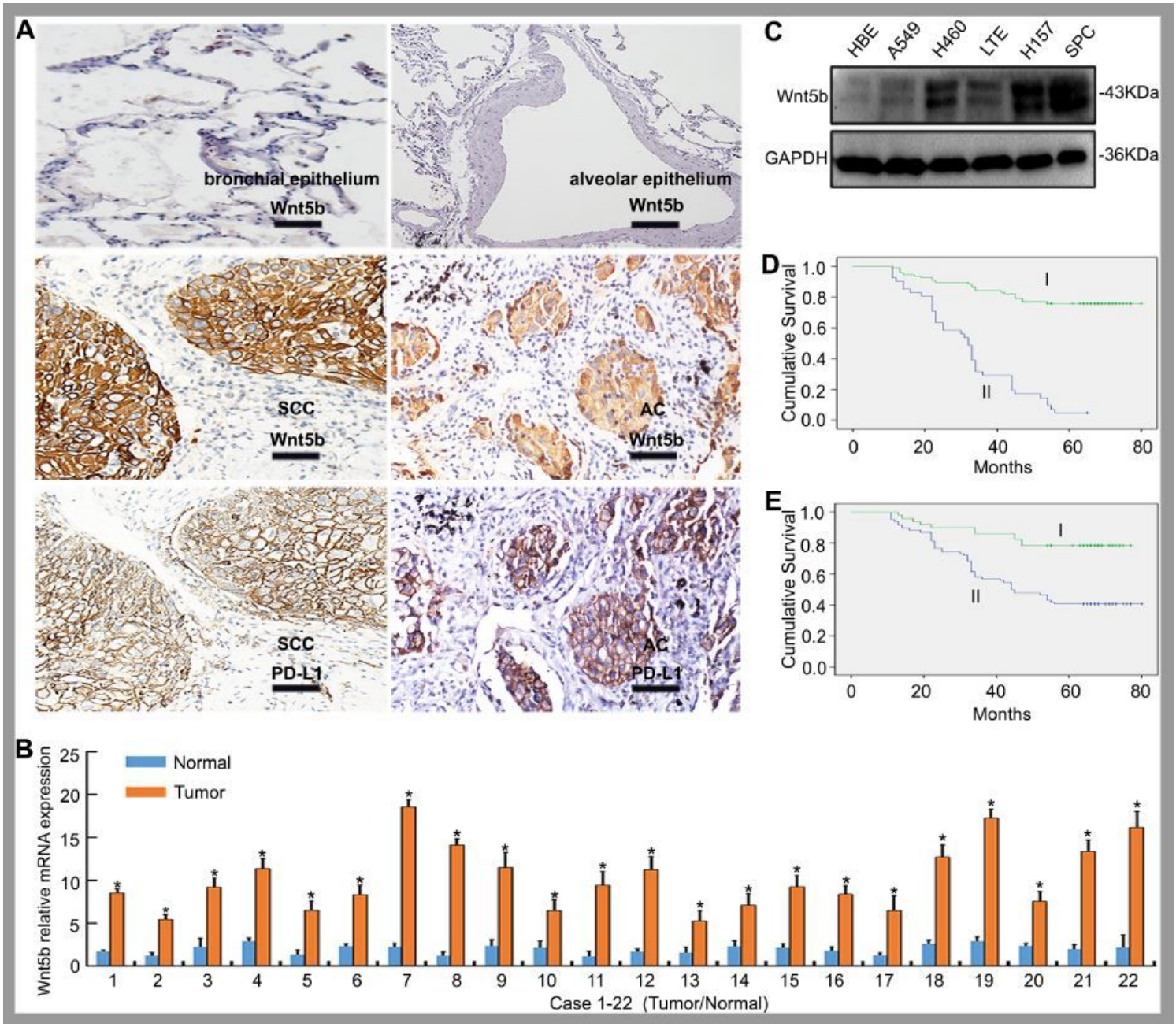

Figure 1

The expression of Wnt5b in NSCLC tissues and cell lines. (a) Wnt5b staining in normal bronchial epithelial cells, alveolar epithelial cells, squamous cell carcinoma (SCC) and adenocarcinoma (AC); PD-L1 staining in SCC and AC (magnification: ×400; scale bar, 20 μm). (b) Quantification of Wnt5b mRNA levels in human NSCLC specimens and paired normal lung tissues by real-time PCR. (c) Wnt5b protein expression in five NSCLC cell lines and the normal bronchial cell line HBE. (d) The survival time of patients with Wnt5b-negative staining (I) and Wnt5b-positive staining (II). (e) The survival time of patients without Wnt5b and PD-L1 coexpression (I) and that of patients with coexpression (II). *, $P<0.05$.

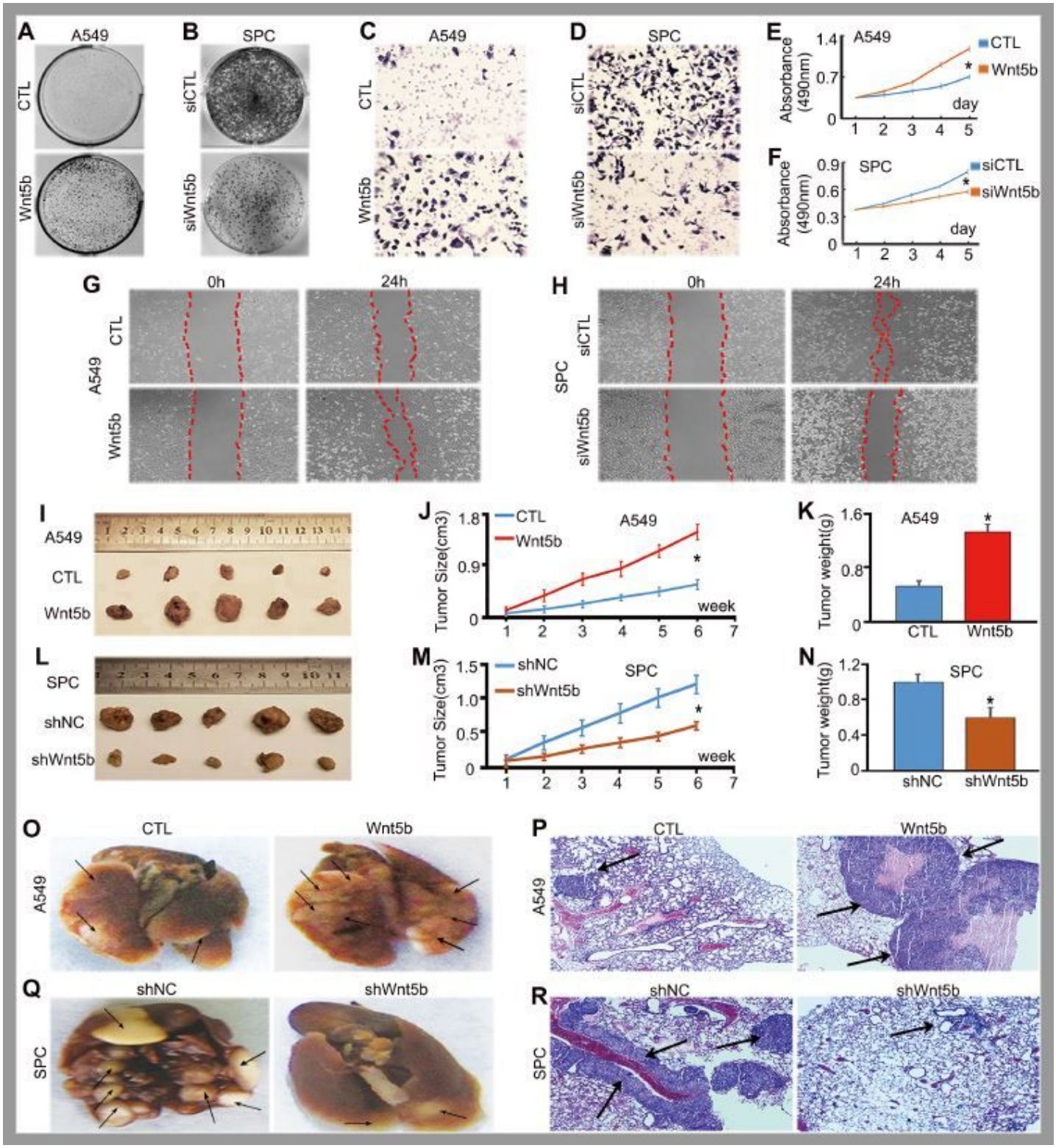

Figure 2

The influence of Wnt5b on the biological behavior of NSCLC cells. Colony formation (a, b), invasiveness (c, d), proliferation (e, f) and migration (g, h) of A549 and SPC cells; CTL, control, empty vector, the control group of Wnt5b expression plasmid. siWnt5b: siRNA-Wnt5b. siCTL, siRNA-control selected as a negative control. (i-n) Subcutaneously injected tumours (G418 screening, n=5). (o-r) Intravenously injection

tumours (G418 screening, n=5). The arrow points to the cancerous area. Columns: mean numbers. shWnt5b, shRNA-Wnt5b. shNC, shRNA-negative control. *, P<0.05.

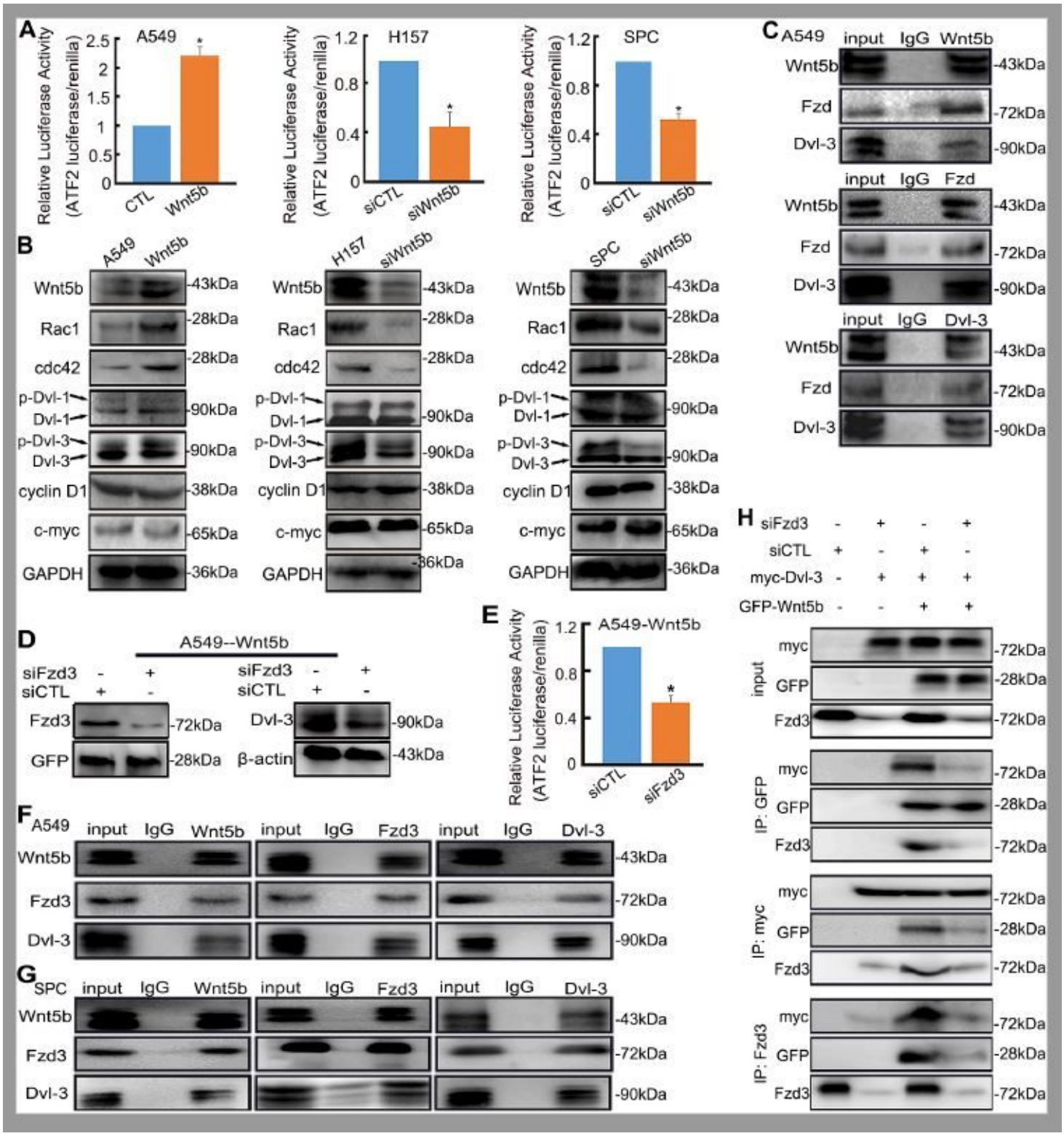

Figure 3

The impact of Wnt5b on the Wnt/PCP pathway. (a) Dual-luciferase assay analyses of Wnt/PCP signaling. Transfection of siRNA-Wnt5b (siWnt5b) or Wnt5b expression plasmid (Wnt5b) to NSCLC cells. ATF2 luciferase was used to measure Wnt/PCP activity, and the values of luciferase activities were normalized

with renilla activity. (b) Western blot analyses of target proteins; transfection of siWnt5b or Wnt5b to NSCLC cells; p-Dvl-1, Dvl-1 phosphorylation; p-Dvl-3, Dvl-3 phosphorylation. (c) Coimmunoprecipitation analyses of endogenous interaction between Wnt5b, Fzd and Dvl-3 in A549. (d) Western blot analyses of Dvl-3 phosphorylation. (e) Dual-luciferase assay analyses of Wnt/PCP signaling; cotransfection of siRNA-Fzd3 (siFzd3) with GFP-Wnt5b. (f-g) Coimmunoprecipitation analyses of endogenous interaction between Wnt5b, Fzd3 and Dvl-3 in A549 and SPC. (h) Coimmunoprecipitation analyses of the interaction of Wnt5b with Dvl-3 in A549; cotransfection of siFzd3 with GFP-Wnt5b and myc-Dvl-3 plasmids. β-actin or GAPDH was selected as a control. siCTL, siRNA-control. *, P <0.05.

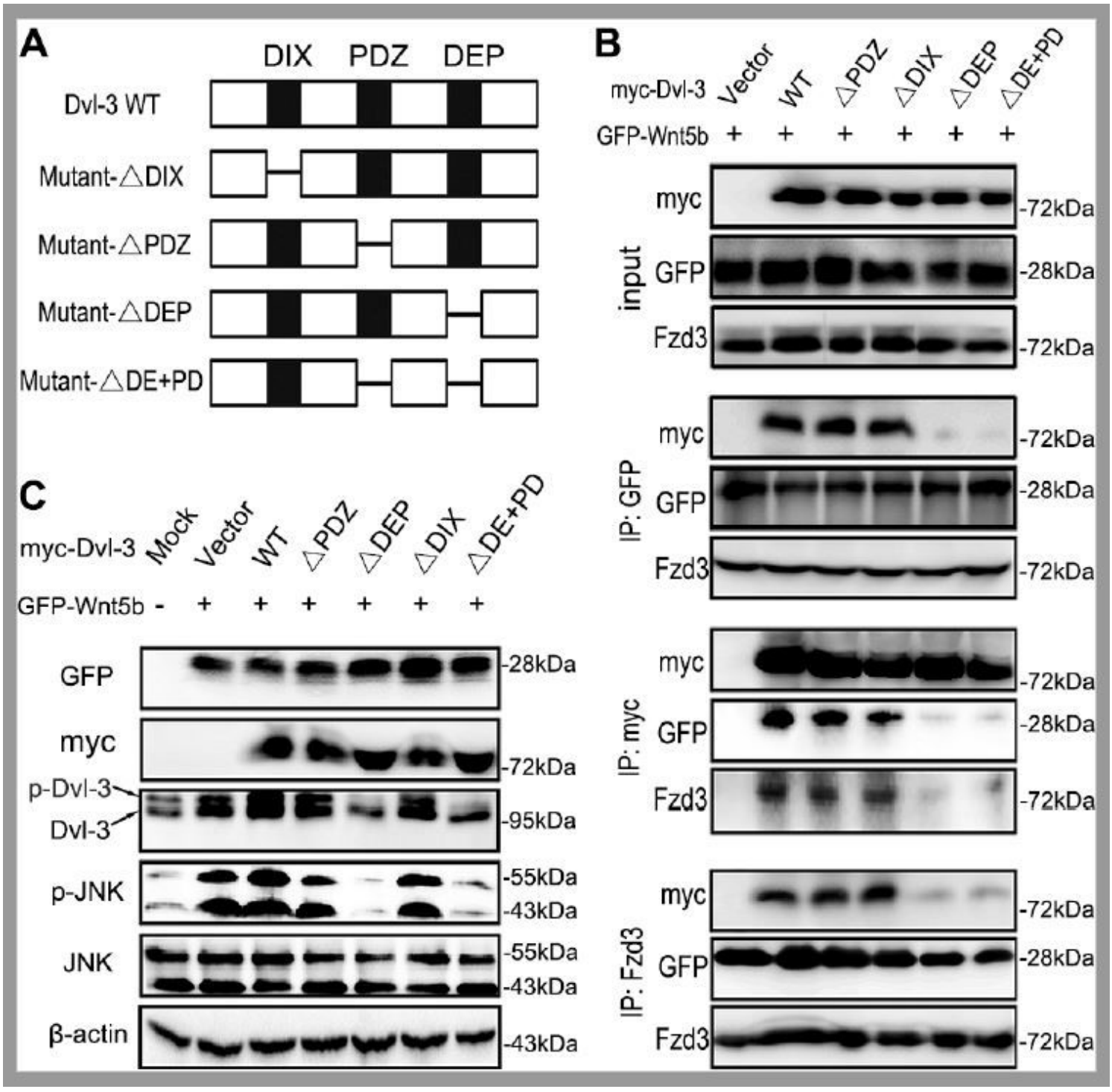

Figure 4

Wnt5b interacted with Dvl-3 DEP domain to promote Dvl-3 phosphorylation and JNK activation. (a) The WT Dvl-3 plasmid and mutant Dvl-3 plasmids (△: this domain deletion). (b) Coimmunoprecipitation analyses of the interaction of Wnt5b with Fzd3 and Dvl-3; the resultant cell lysates were immunoprecipitated with GFP/myc/Fzd3 antibody; the presence of Wnt5b/Dvl-3/Fzd3 was confirmed by anti-GFP/myc/Fzd3 immunoblotting. (c) Western blot analyses of Dvl-3 and JNK. Cotransfection of GFP-Wnt5b with WT myc-Dvl-3 or Dvl-3 mutant plasmids to A549 cell; p-Dvl-3, Dvl-3 phosphorylation; p-JNK, JNK phosphorylation. β-actin was selected as a negative control. △DE+PD: △DEP+PDZ.

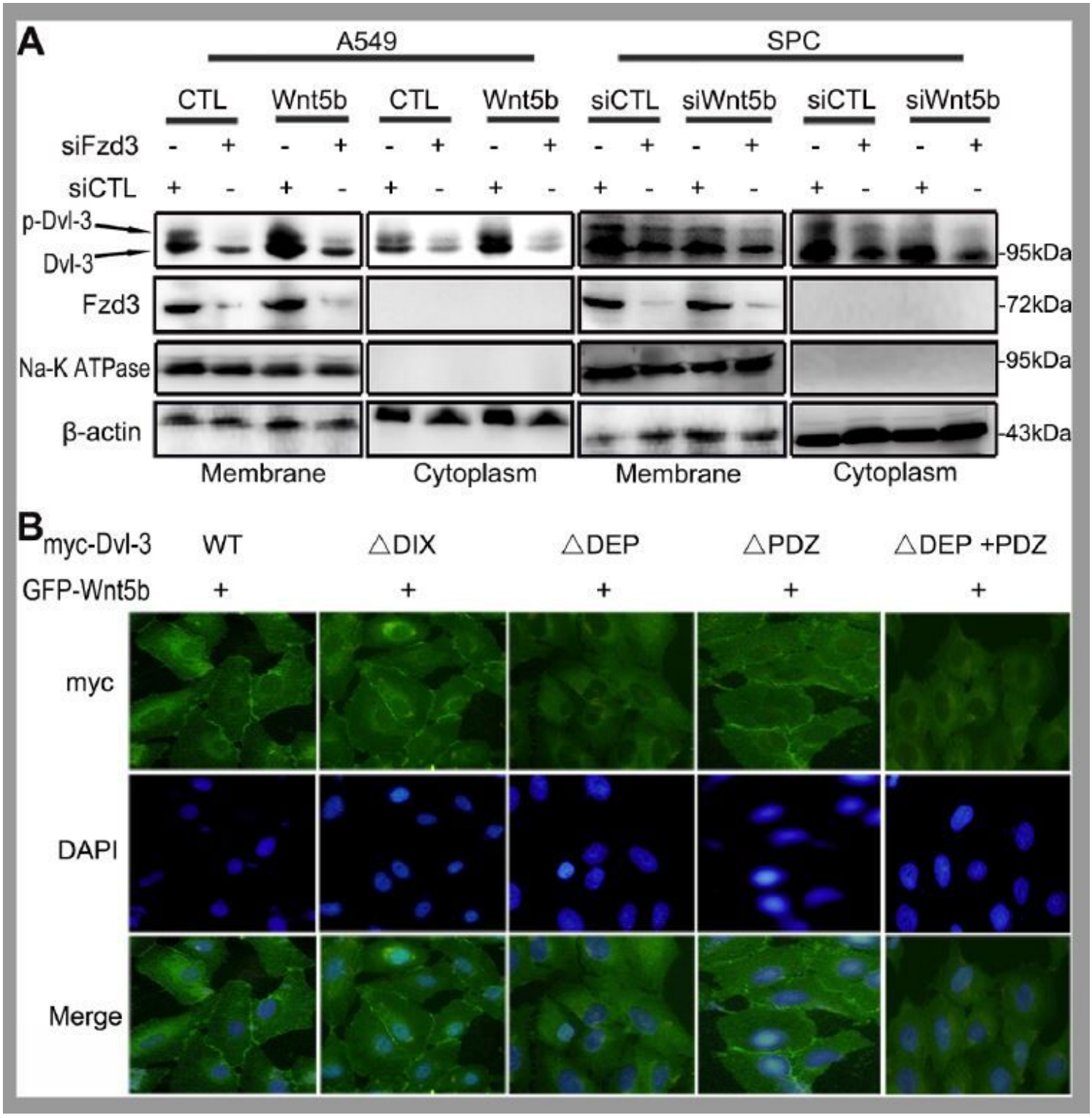

Figure 5

The effect of Wnt5b on Dvl-3 membrane recruitment. (a) Western blot analyses of Dvl-3 phosphorylation on cell membrane and cytoplasm; cotransfection of siRNA-Fzd3 (siFzd3) with Wnt5b expression plasmid (Wnt5b) to A549 or siRNA-Wnt5b (siWnt5b) with Wnt5b to SPC for 48 h. CTL, control, empty vector, the control group of Wnt5b expression plasmid; siCTL, siRNA-control. p-Dvl-3, Dvl-3 phosphorylation. Na-K ATPase was a reference control for membrane. (b) Analysis of Dvl-3 localization with confocal microscopy (magnification: ×400); cotransfection of GFP-Wnt5b with WT myc-Dvl-3 or Dvl-3 mutant plasmids for 48 h to A549 cell.

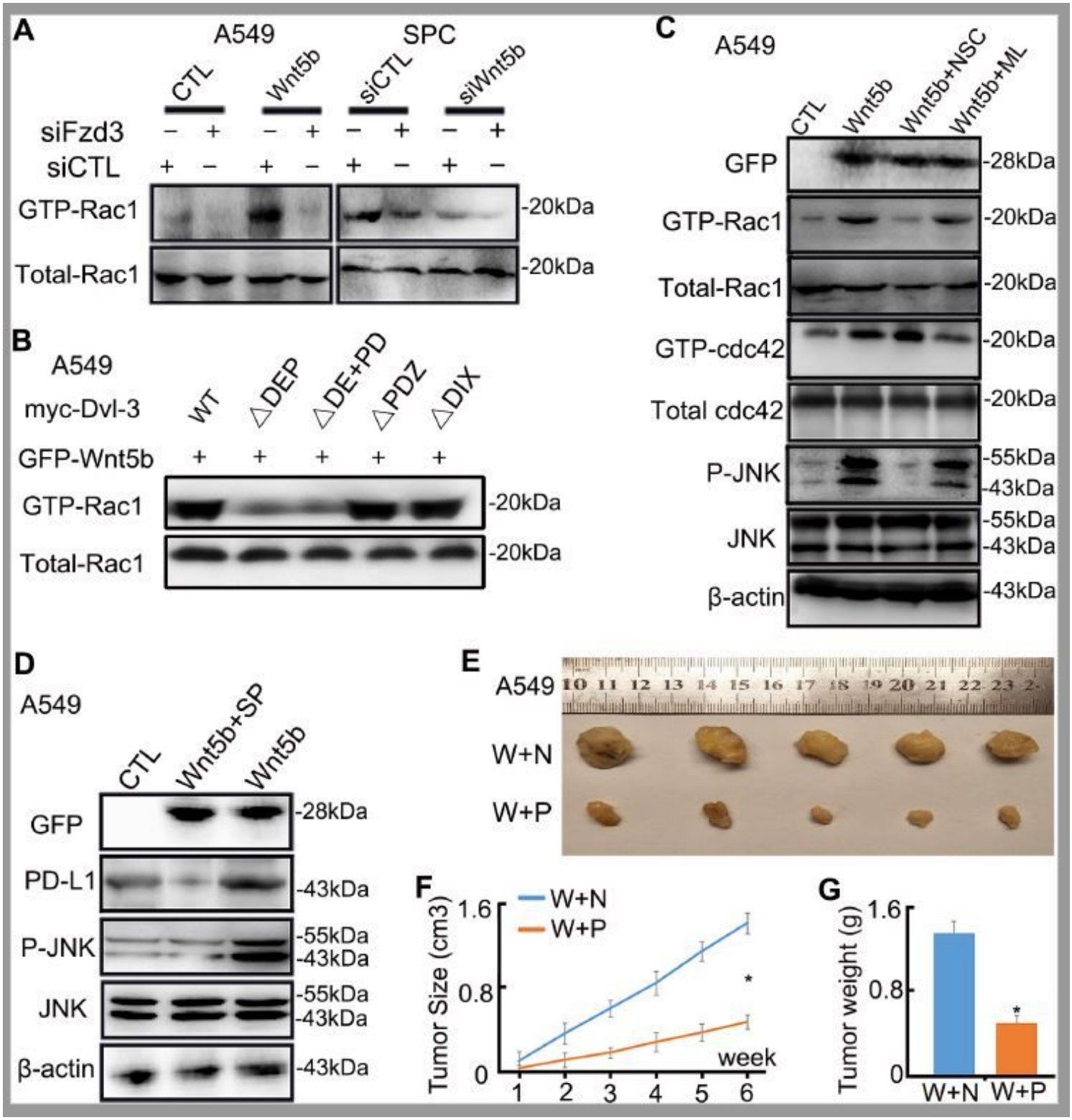

Figure 6

The impact of Wnt5b on Rac1, JNK and PD-L1. (a) Western blot analyses of activated Rac1; cotransfection of siRNA-Fzd3 (siFzd3) with Wnt5b expression plasmid (Wnt5b) or siRNA-Wnt5b (siWnt5b). (b) Western blot analyses of Rac1 in A549 cell; cotransfection of GFP-Wnt5b with WT myc-Dvl-3 or Dvl-3 mutant plasmids. (c) Western blot analyses of Rac1, cdc42 and JNK. P-JNK, JNK phosphorylation; transfection of GFP-Wnt5b (Wnt5b) to A549 cell. After Wnt5b transfection, NSC23766 (a Rac1 inhibitor, 100 μM, Wnt5b+NSC) or ML141 (a cdc42 inhibitor, 10 μM, Wnt5b+ML141) was treated for 24 h. Whole-cell lysates were run on parallel gels to determine total Rac1 or cdc42. (d) Western blot analyses of PD-L1 and JNK; transfection of GFP-Wnt5b (Wnt5b) to A549. After Wnt5b transfection, SP600125 (JNK inhibitor, 10 μM, Wnt5b+SP) was treated for 24 h. (e-g) Subcutaneously injected tumours of A549 cell stably expressing Wnt5b (G418 screening, n=5) with PD-L1 antibody treatment. CTL, control, empty vector, the control group of Wnt5b expression plasmid; siCTL, siRNA-control. β-actin was selected as a negative control. W+N, Wnt5b+negative control for PD-L1 antibody; W+P, Wnt5b+PD-L1 antibody. *, $P < 0.05$.

Supplementary Files

This is a list of supplementary files associated with this preprint. Click to download.

- Additionalfile13Fig.S11.pdf
- Additionalfile13Fig.S11.pdf
- Additionalfile12Fig.S10.pdf
- Additionalfile12Fig.S10.pdf
- Additionalfile11Fig.S9.pdf
- Additionalfile11Fig.S9.pdf
- Additionalfile10Fig.S8.pdf
- Additionalfile10Fig.S8.pdf
- Additionalfile9Fig.S7.pdf
- Additionalfile9Fig.S7.pdf
- Additionalfile8Fig.S6.pdf
- Additionalfile8Fig.S6.pdf
- Additionalfile7Fig.S5.pdf
- Additionalfile7Fig.S5.pdf
- Additionalfile6Fig.S4.pdf
- Additionalfile6Fig.S4.pdf
- Additionalfile5Fig.S3.pdf
- Additionalfile5Fig.S3.pdf

- Additionalfile4Fig.S2.pdf
- Additionalfile4Fig.S2.pdf
- Additionalfile3Fig.S1.pdf
- Additionalfile3Fig.S1.pdf
- Additionalfile2TableS2.doc
- Additionalfile2TableS2.doc
- Additionalfile1TableS1.doc
- Additionalfile1TableS1.doc
- Supplementaryfiles.doc
- Supplementaryfiles.doc